MULTIFUNCTIONAL LPBF-MANUFACTURED HEAT SINKS WITH INTEGRATED PARTICLE DAMPERS FOR SHOCK MITIGATION IN ELECTRONICS

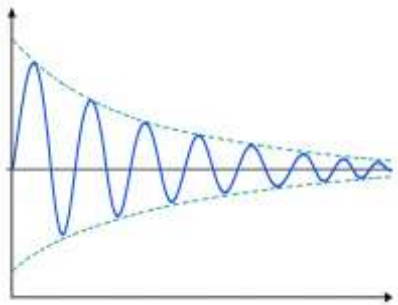
Digambar Killedar[a], Joud N Satme[a], Mohsen Gol Zardian[a], Trotter Roberts[a], Patrick Wynne[a],Austin R.J. Downey[a, b], Yanzhou Fu[c], and Lang Yuan[a]

[a] Department of Mechanical Engineering, University of South Carolina, Columbia, SC, USA

[b] Department of Civil and Environmental Engineering, University of South Carolina, Columbia, SC, USA

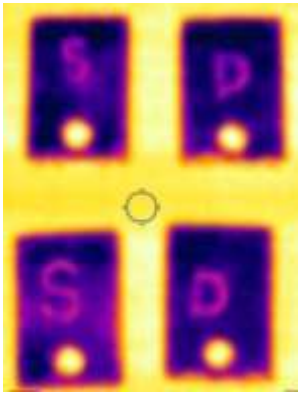
[c] Department of Ocean and Mechanical Engineering, Florida Atlantic University, Boca Raton, FL, US

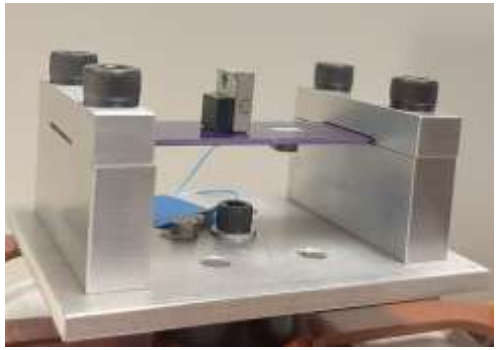




UNIVERSITY OF South Carolina

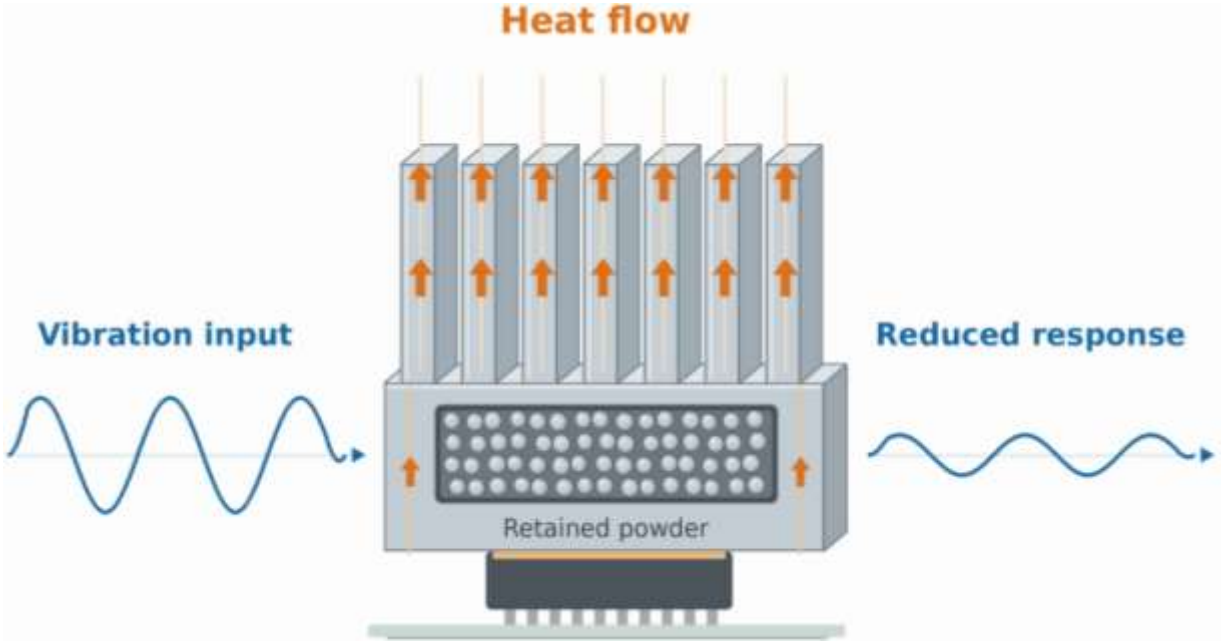
Molinaroli College of Engineering and Computing





Outline

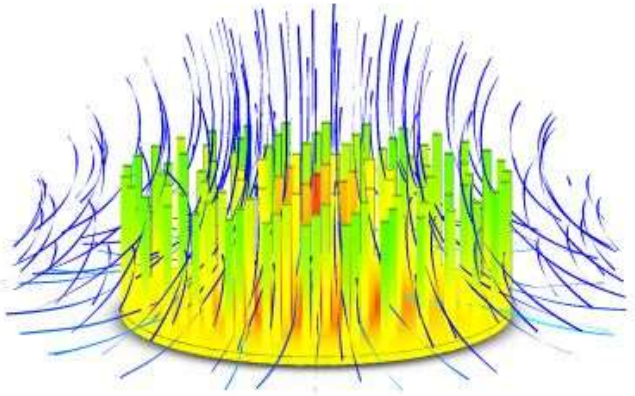
- Heat Sink Design
- Thermal Study
- Vibration Study
- Shock Study
- Closing Remarks and Future Efforts



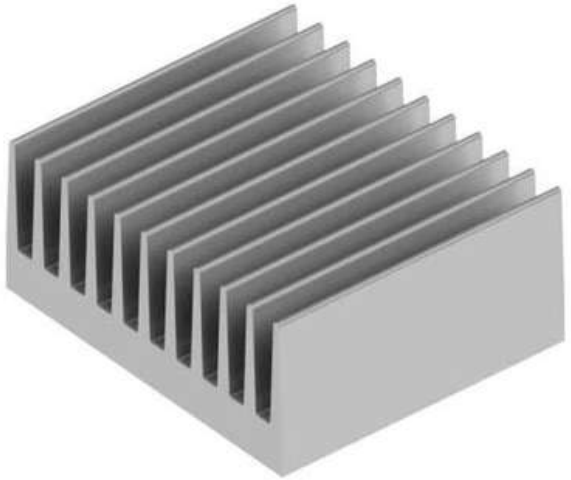
Heat sink with an integrated particle damper

Heat Sinks in Electronic Assemblies

- Electronic components generate heat.
- Heat sinks conduct heat away from components.
- Fins increase the surface area for cooling.
- Electronic assemblies also experience shock and vibration.



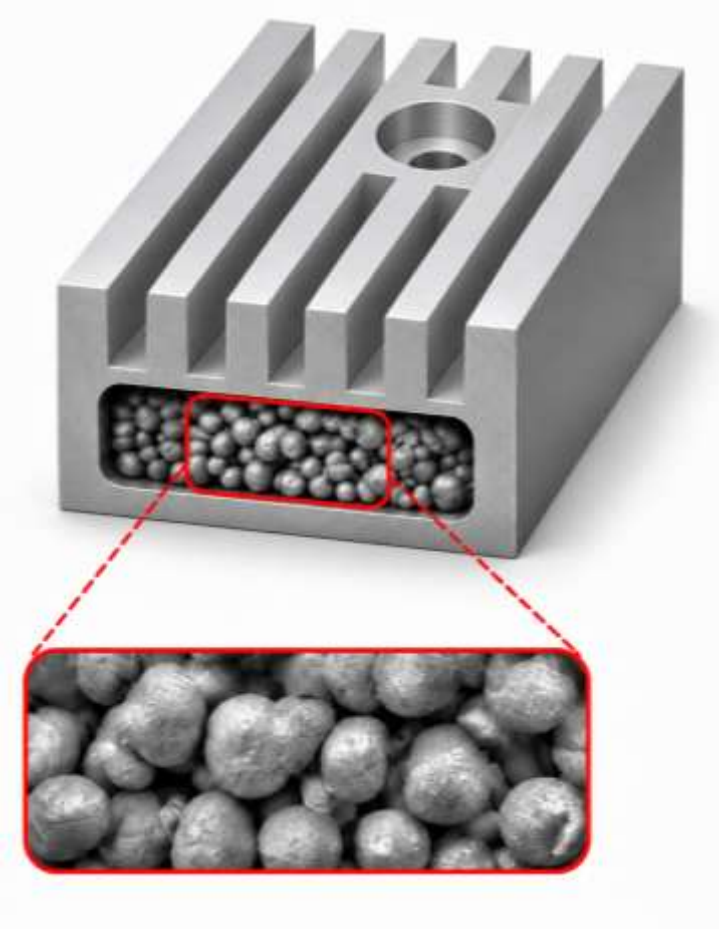
User:Isofilm, CC BY-SA 3.0, via Wikimedia Commons

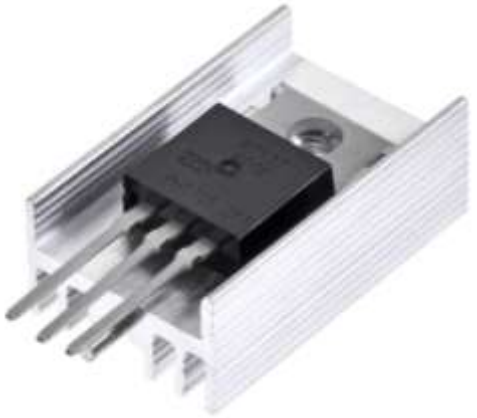


https://www.digikey.com/

Particle Damping in Heat Sinks

- Loose particles are contained within an internal cavity.
- Collisions and friction dissipate mechanical energy.
- Damping depends on particle packing and available motion.
- A heat sink can provide both cooling and passive damping.





Walmart.com



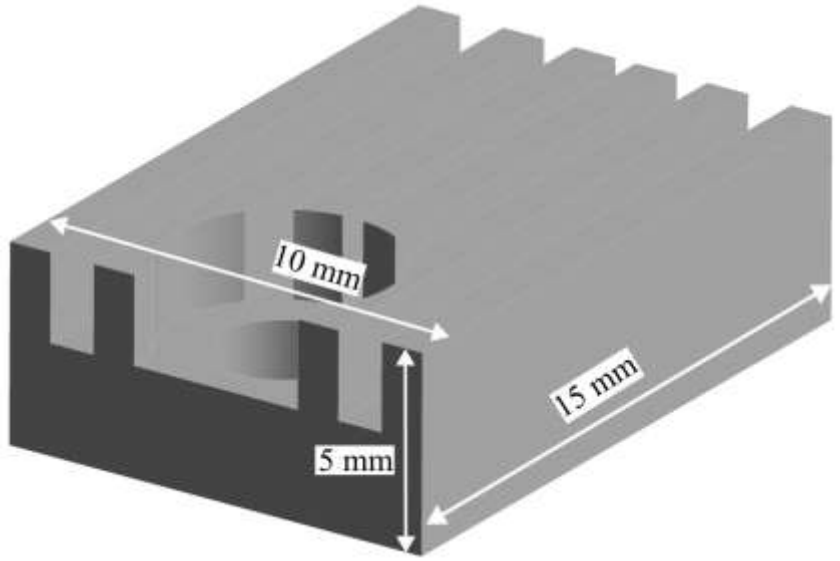
hv-experimental.com

Heat Sink Design

Heat Sinks with Integrated Particle Dampers

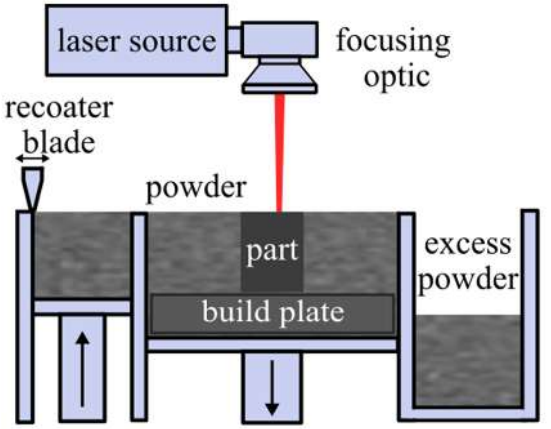
- Geometry adapted from a commercial MOSFET heat sink.
- External dimensions of 15 × 10 × 5 mm.
- Fabricated in 316L stainless steel using LPBF.
- Solid and retained-powder versions produced for comparison.

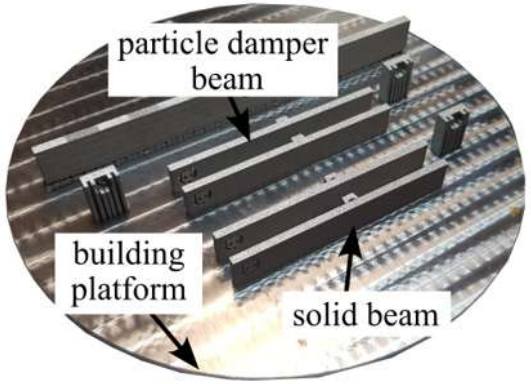


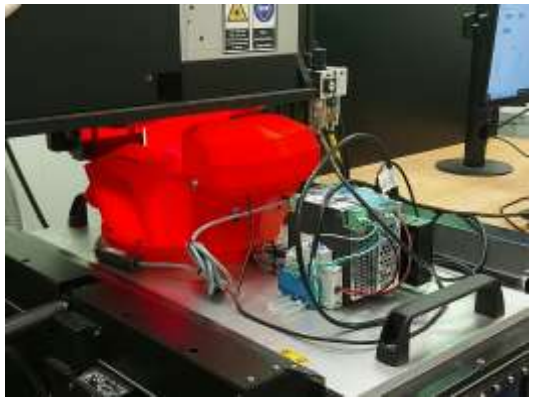


LPBF Printing

- Aconity3D MIDI system using 316L stainless steel powder under an argon atmosphere.
- Laser power of 150 W and scan speed of 800 mm/s.
- Hatch spacing of 0.10 mm and layer thickness of 30 μm.
- Solid and particle-damper heat sinks fabricated at a volumetric energy density of 62.5 J/mm³.







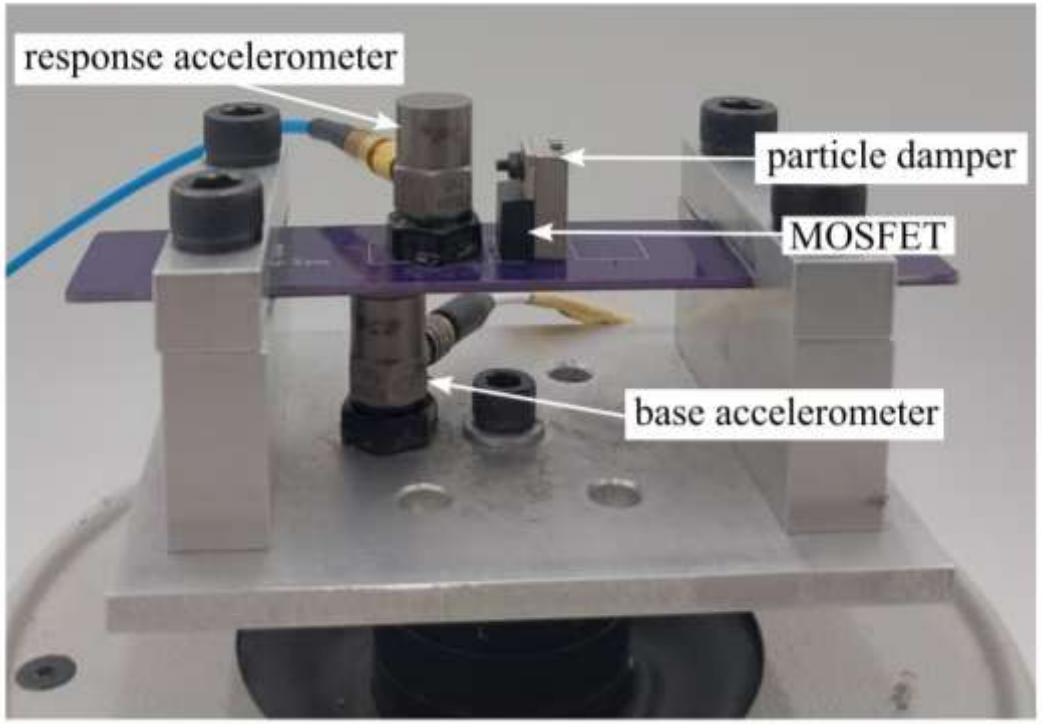


Element	Iron	Ni	Cr	O	Si	S	P	N	C	Mo	Mg	Cu
Weight percent (%)	Bal.	12.7	17.7	0.03	0.62	0.01	0.01	0.10	0.02	2.36	0.65	0.02

Nominal chemical composition of stainless steel 316L, expressed in weight percent (%)

Free Vibration Tap Test

- Fixed–fixed PCB assembly excited using a short and light tap from a screwdriver tip.
- Accelerations measured at the PCB.
- Test undertaken to find the natural frequency of the system.

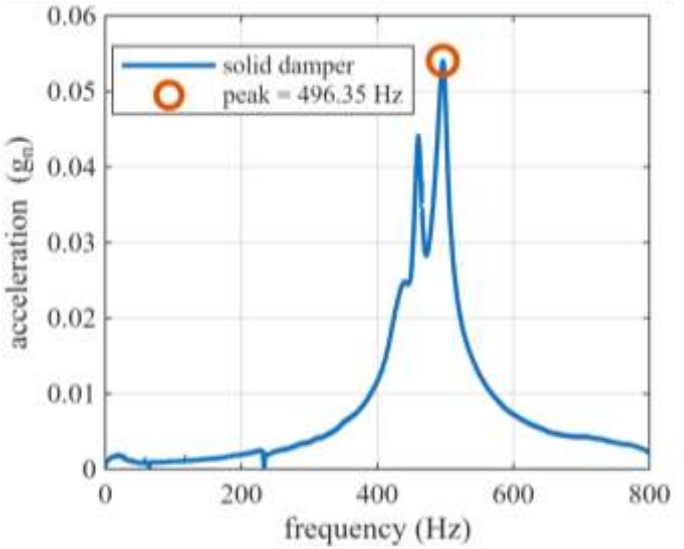




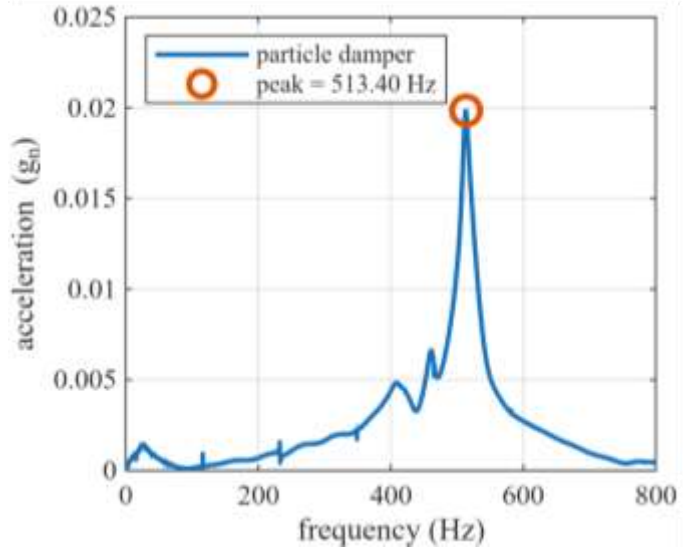
Natural Frequency Comparison

- Solid heat-sink configuration: 496.35 Hz.
- Particle-damper configuration: 513.40 Hz.
- Frequency increases by 17.05 Hz, approximately 3.4%.
- Both configurations retain a dominant frequency near 500 Hz.

Solid Damper



Particle Damper



Thermal Study

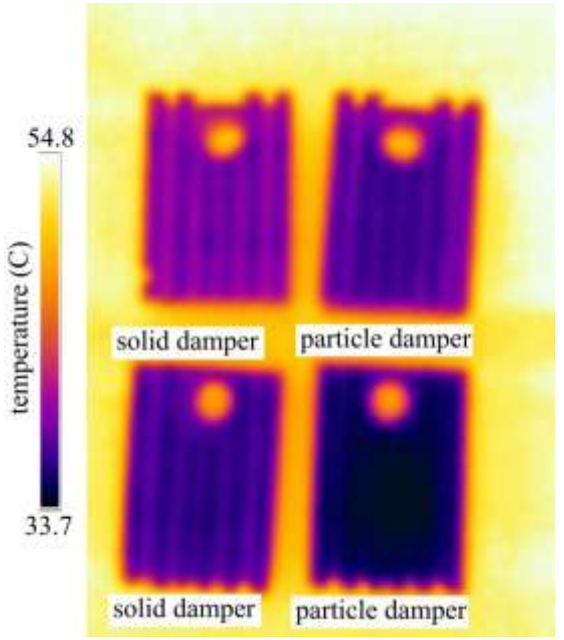
Infrared thermal testing procedure

- Solid and particle-damper heat sinks heated on a controlled bed at 60 °C.
- FLIR infrared camera records surface temperature distributions during heating.
- Thermal images compared after 1 minute and 5 minutes.
- Camera position, viewing angle, and ambient conditions held constant between configurations.

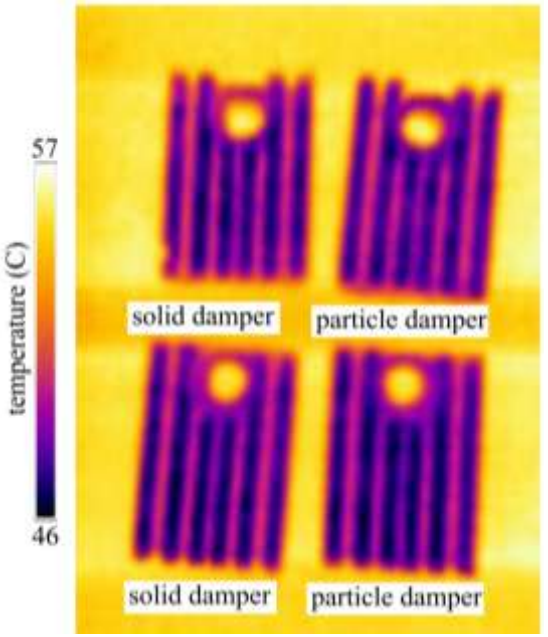


Thermal conductivity comparison

- Thermal imaging suggests comparable heat-sink behavior after the transient heating period.
- A qualitative comparison is carried out to demonstrate the effect of the particle cavity on heat conduction.
  - At 1 min: a cooler cavity region (~34 °C) is observed at the particle damper due to reduced conduction.
  - At 5 min: similar temperature distributions.
- The rate of heat conduction is affected by the porous particle cavity in the particle damper.



1 min

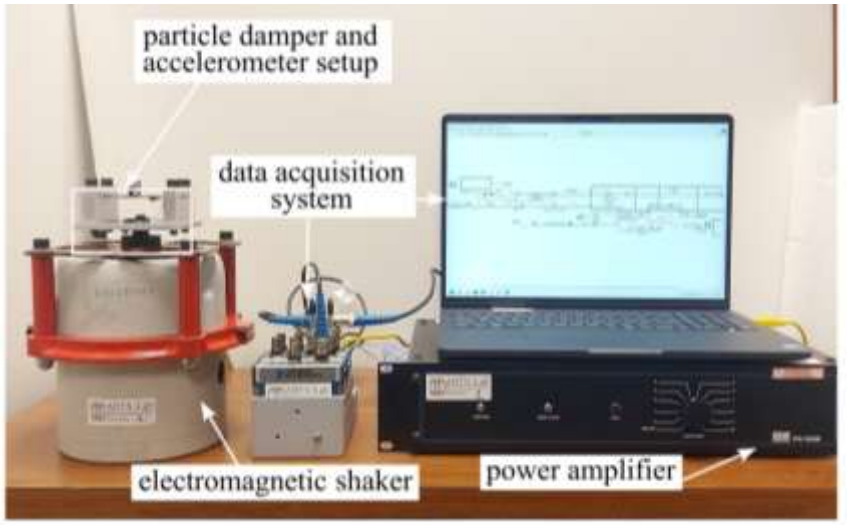


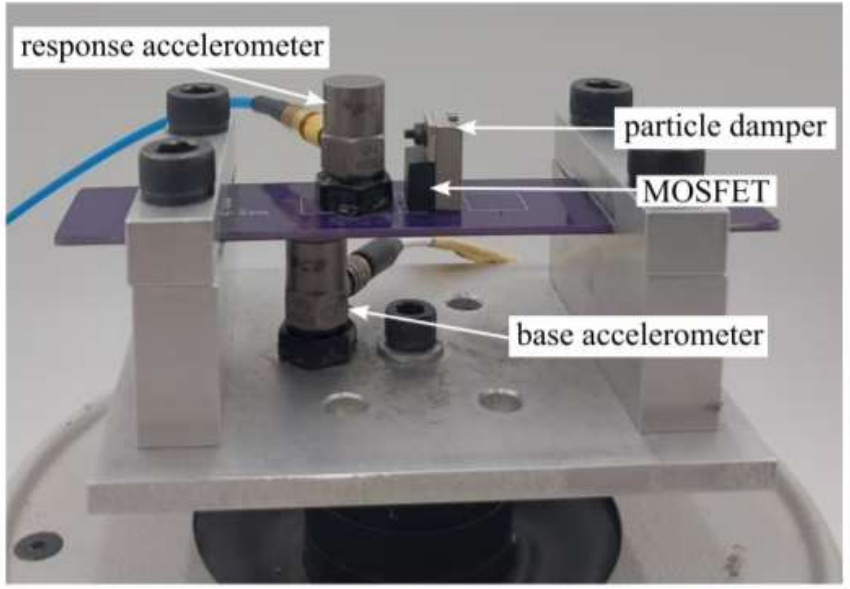
5 min

Vibration Test

Forced Vibration Testing

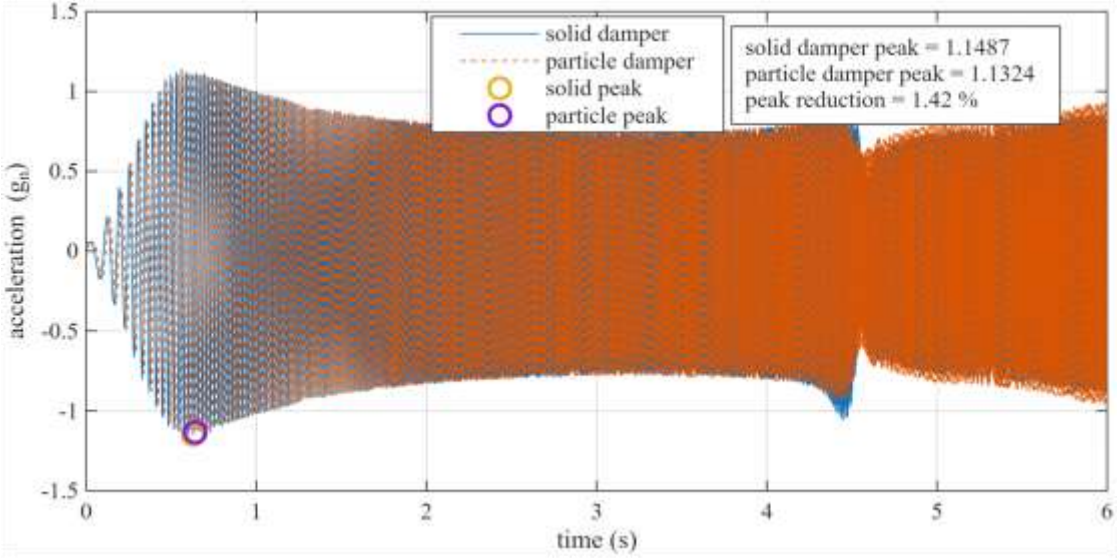
- Fixed–fixed PCB assembly excited using an electromagnetic shaker.
- Swept-sine base excitation applied over 400–650 Hz.
- Accelerations measured at the excitation input, structural base, and PCB.
- FFT and PCB-to-base transmissibility evaluated, including the 465–520 Hz resonant band.





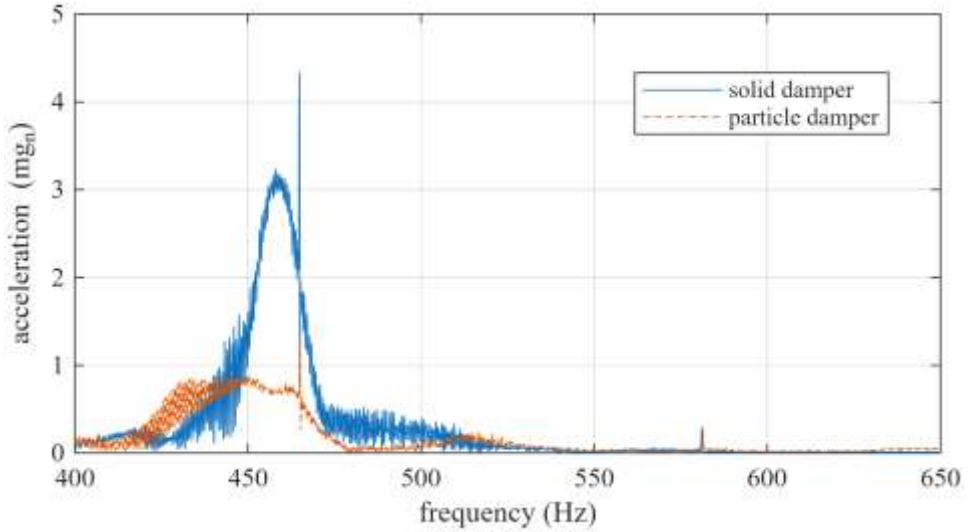
Force Vibration Time Histories

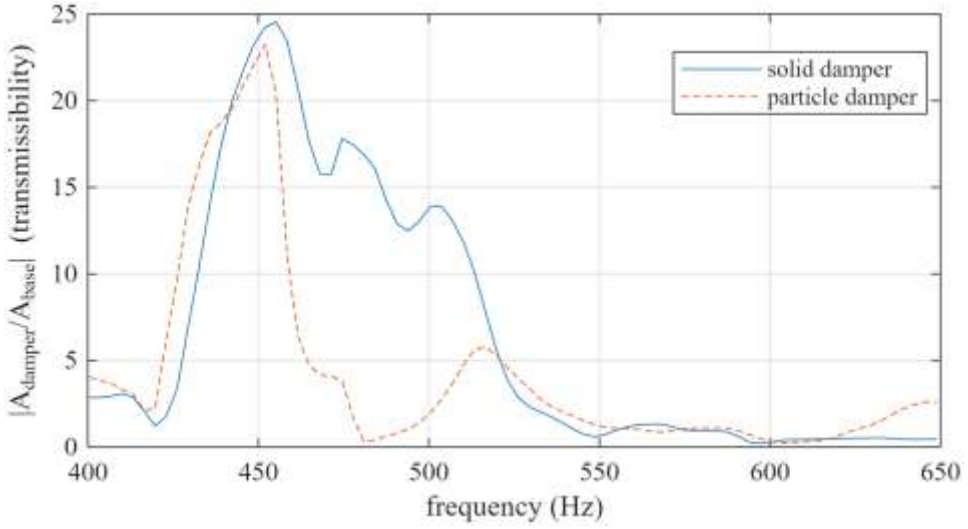
- The forced vibration test takes the system through resonance (~500 Hz) at 4.5 seconds into the test.
- PCB acceleration was recorded for both heat-sink designs.
- FFT of each response was used to identify the dominant frequency.



Frequency Response and Transmissibility

- Swept-sine excitation spans 400–650 Hz.
- Particle-damper heat sink reduces the peak PCB FFT amplitude by 71.8%.
- Transmissibility shows reduced amplification across much of the resonant region.
- Integrated squared transmissibility decreases by 34.9% over the test band.





Vibration Performance Summary

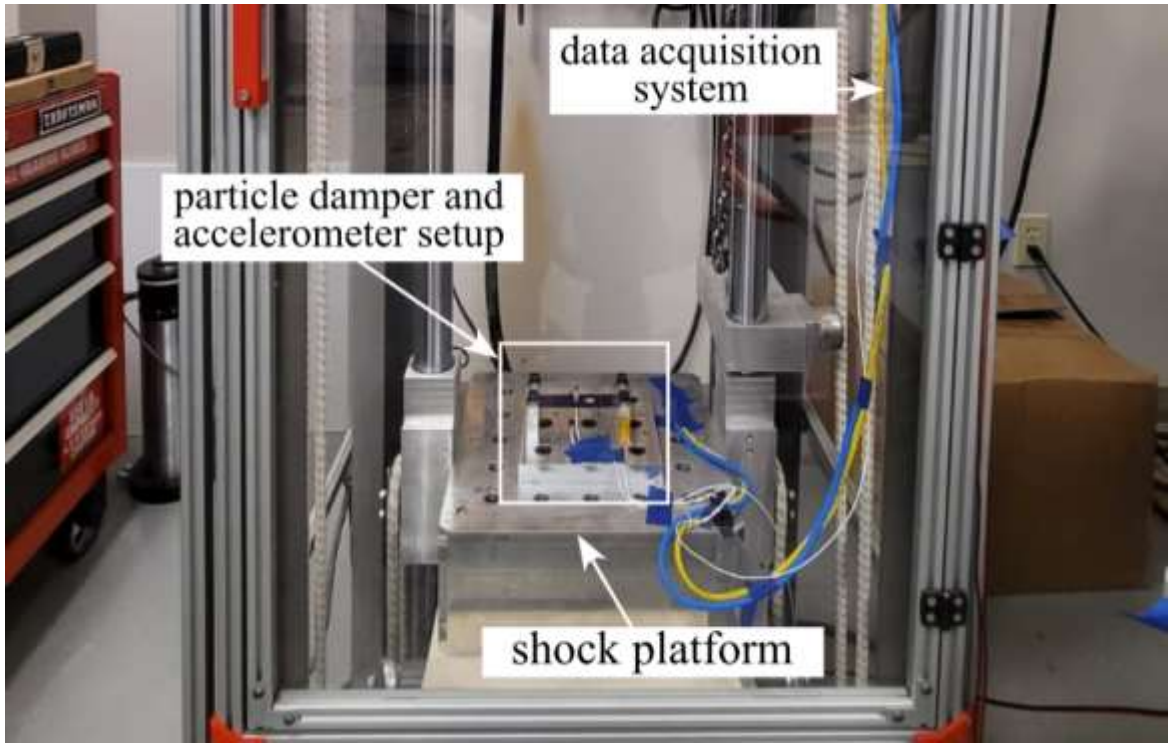
- The particle-damper heat sink reduced
  - the peak FFT amplitude by 72%
  - the integrated squared transmissibility by 35%.
- Changes to the peak acceleration and dominant frequency were minimal.

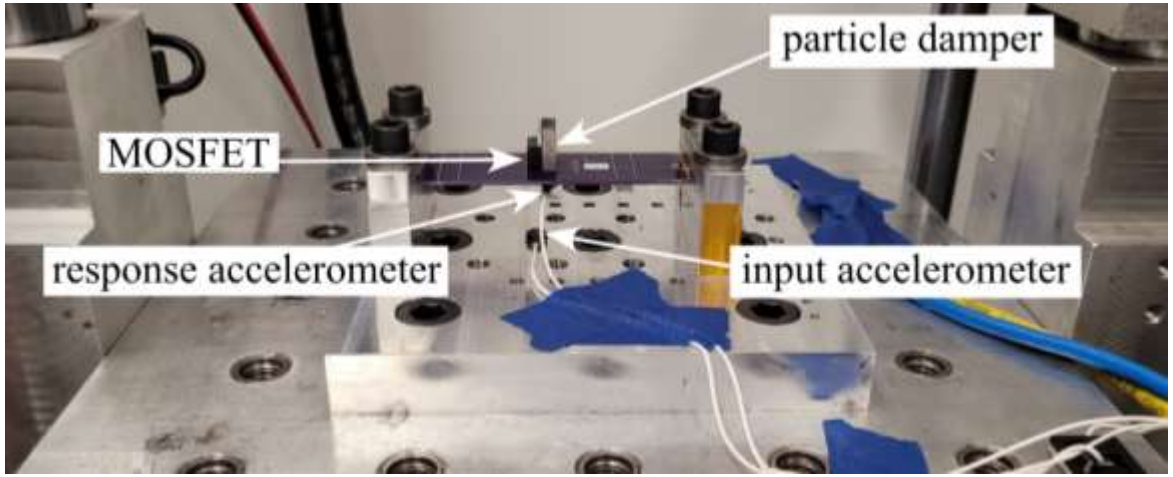
Metric	Solid	Particle	Change
Peak PCB acceleration (g_n)	1.1487	1.1324	−1.42%
FFT peak amplitude	4.336×10^{-3}	1.222×10^{-3}	−71.81%
Spectral response index, 465–520 Hz	4.821×10^{-5}	4.937×10^{-6}	−89.76%
Integrated squared transmissibility (T^2)	2.845×10^{4}	1.853×10^{4}	−34.87%

Shock Study

Shock Testing

- Fixed–fixed PCB assembly with the heat sink attached to the centrally mounted MOSFET.
- Hydraulic drop-table excitation applied to solid and particle-damper configurations.
- Accelerometers record input and PCB response accelerations in g_n.
- Free decay evaluated using damping ratio, decay constant (s^{-1}), and settling time to 5% amplitude (ms).





Quantifying Time-domain Shock Attenuation

- Response of both damper configurations is plotted in terms of acceleration versus time, and the positive peaks are identified to evaluate the decay and vibration attenuation behavior.

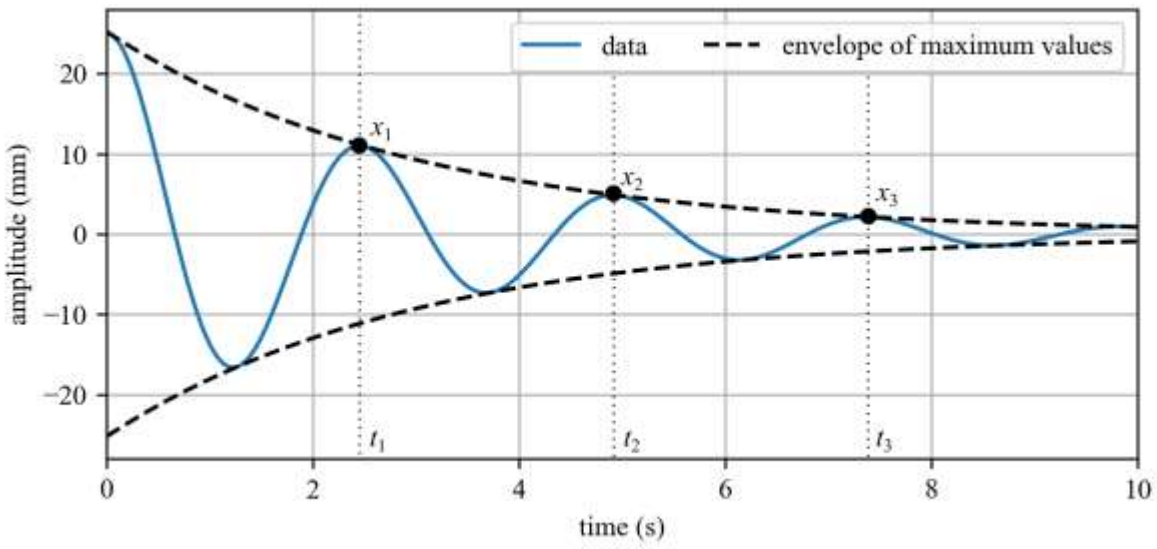
$$\delta = \frac{1}{n} \ln \left(\frac{x_i}{x_{i+n}} \right)$$

- The damping ration is.

$$\zeta = \frac{\delta}{\sqrt{4\pi^2 + \delta^2}}$$

- An exponential decay fit is included to represent the vibration attenuation trend after the initial shock event.

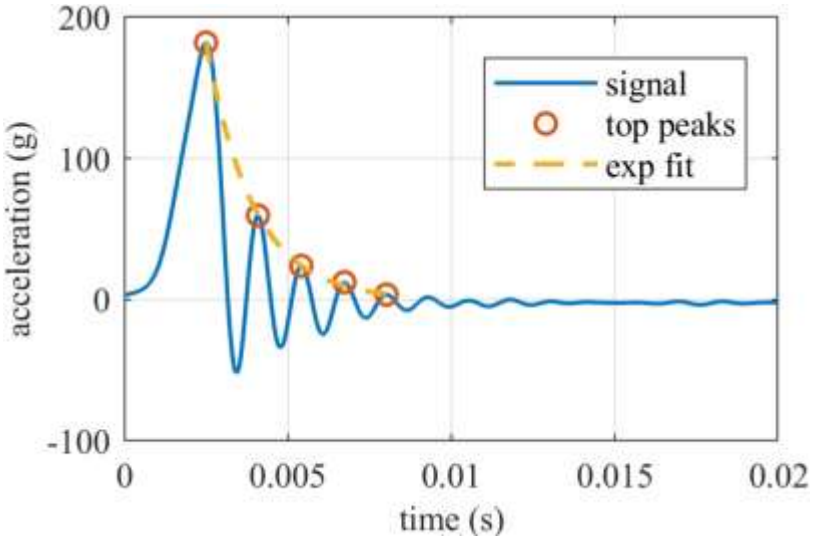
$$y = Ae^{-\zeta \omega_n t}$$



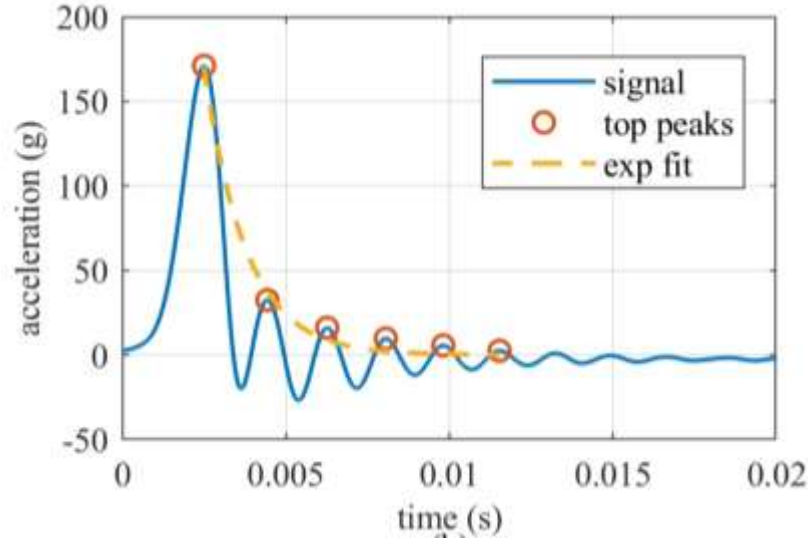
Measured Acceleration Histories

- Initial peaks were similar:
  - Initial peak: 182.0 → 171.0 g_n (−6.0%).
  - Second peak: 59.56 → 32.43 g_n (−45.5%).
- After the initial peak, the particle-damper response decayed faster.

Solid Damper

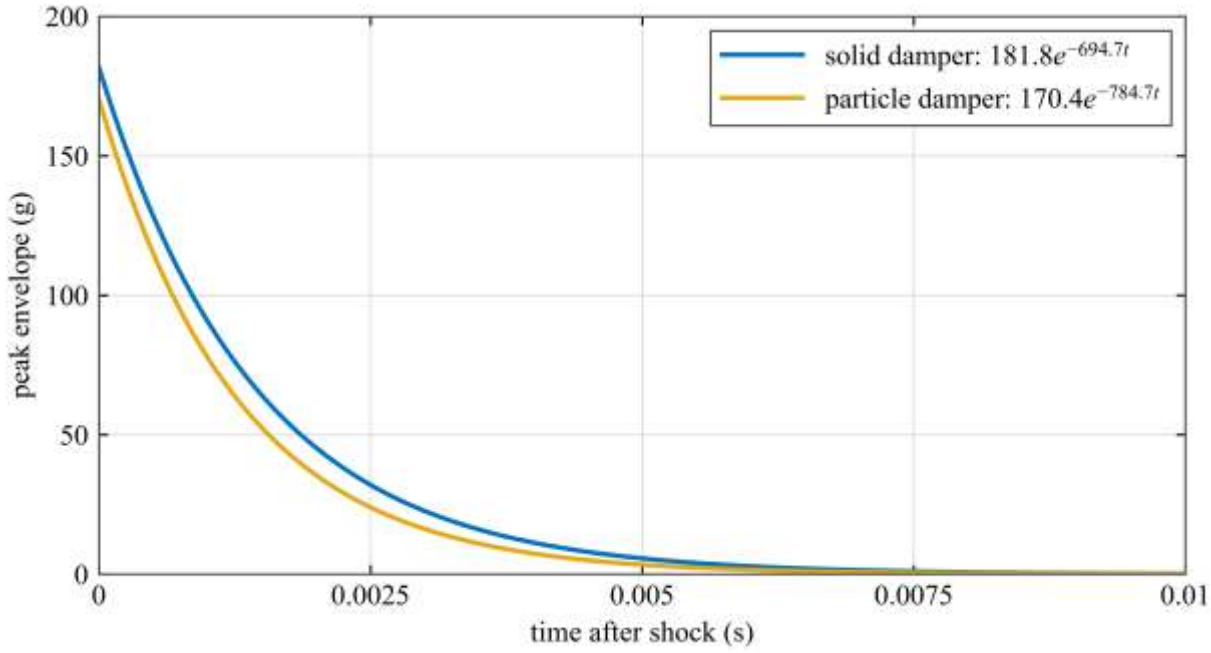


Particle Damper



Measured Envelopes

- Solid heat sink decay constant: 694.7 s^{-1}.
- Particle-damper decay constant: 784.7 s^{-1}, about 13% higher.
- The higher decay constant indicates that the vibration amplitude decays faster after the initial shock.



Shock Attenuation Results

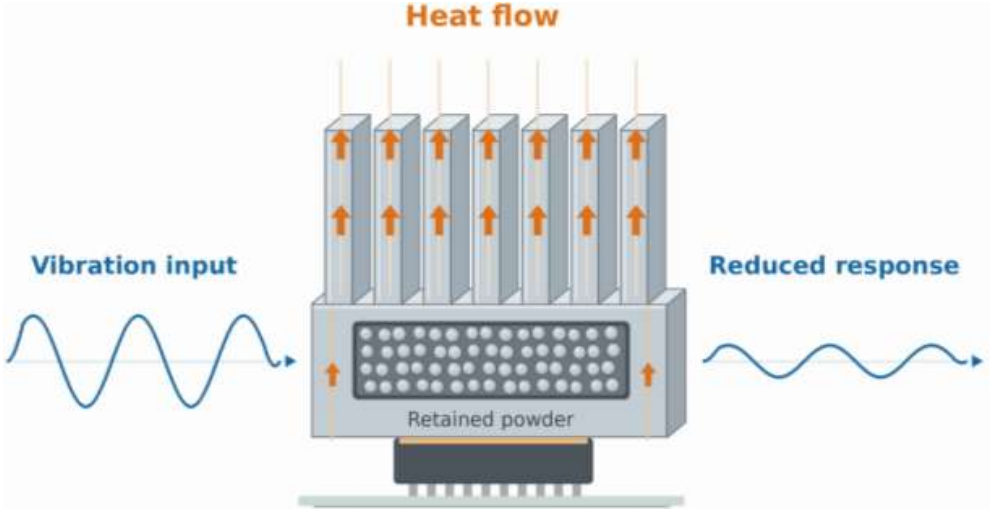
- Peak acceleration decreased by 6.0%, from 182.0 to 171.0 g_n.
- The second peak fell by 45.5%, from 59.56 to 32.43 g_n, showing a much smaller response after the initial shock.
- Estimated damping ratio increased 46.0% (0.151 to 0.220), while settling time to 5% amplitude decreased 11.5% (4.3 to 3.8 ms).

Metric	Solid	Particle Damper	Improvement
Peak acceleration (g)	182.0	171.0	6.04% ↓
Second peak (g)	59.56	32.43	45.54% ↓
Decay constant, λ	694.7	784.7	12.96% ↑
Estimated damping ratio, ζ	0.151	0.220	46.01% ↑
Settling time to 5% amplitude (s)	0.0043	0.0038	11.47% ↓

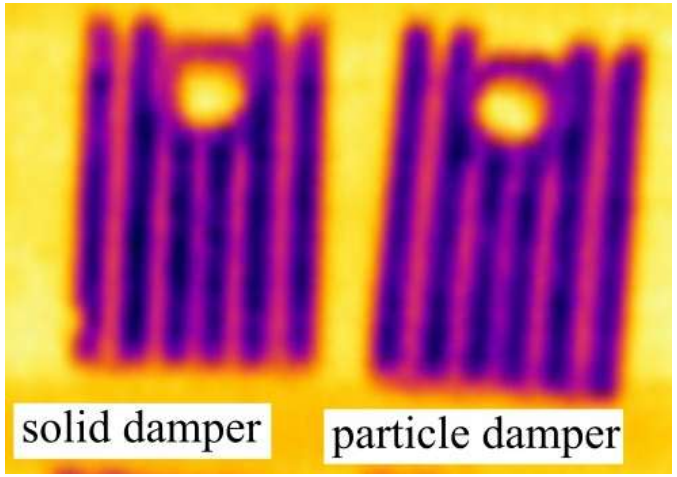
Closing Remarks and Future Efforts

Closing Remarks and Future Efforts

- Potential for high-power aerospace, automotive, and defense electronics.
- Shock peaks decreased 6% initially and 45.5% at the second response peak; test whether prior vibration further reduces the initial peak.
- Quantify heat transfer through particle-to-particle contacts.







Acknowledgement

This This research was supported by the United States National Science Foundation (NSF), USA, Grants Nos.CCF-2503055, and CPS-2237696. This work is also partially supported by the National Institute of Standards & Technology, United States, under grant number 70NANB23H030, as well as the South Carolina Space Grant Consortium under grants 21-117-RID RGP-SC-009, 25-073-REAP-SC-001, and 25-073-BTC-SC-001. Additional support is provided by the United States' National Science Foundation (NSF) through the NSF ASEE Fellowship. Any opinions, findings, conclusions, or recommendations expressed in this material are those of the authors and do not necessarily reflect the views of the National Science Foundation, the South Carolina Space Grant Consortium, or the National Institute of Standards & Technology.







Discussion

ARTS-Lab

github.com/Arts-laboratory



Name: Dr. Austin R. J. Downey
Email: austindowney@sc.edu



Molinaroli College of Engineering and Computing
UNIVERSITY OF SOUTH CAROLINA

References

- Joud N Satme, Yanzhou Fu, Samuel Roberts, Austin R J Downey, Tianyu Zhang, Lang Yuan, and Daniel Kiracofe. Tunable shock and vibration damping in metal laser powder bed fusion components via controlled post-print compaction of particle damper cavities. Smart Materials and Structures, 35(4):045015, April 2026. doi:10.1088/1361-665x/ae59d7
- Joud N. Satme, Yanzhou Fu, Austin R. Downey, Lang Yuan, and Daniel Kiracofe. Impact of particle packing density on the frequency response of an additively manufactured particle damper. In *AIAA SCITECH 2024 Forum*. American Institute of Aeronautics and Astronautics, January 2024. doi:10.2514/6.2024-0024
- Yanzhou Fu, Satme Joud, Austin R. J. Downey, Lang Yuan, Tianyu Zhang, and Daniel Kiracofe. Investigating compressing particle damper pockets in beams manufactured by laser powder bed fusion additive manufacturing. In Special Topics in Structural Dynamics & Experimental Techniques, Volume 5, pages 139-144. Springer Nature Switzerland, jun 2023. doi:10.1007/978-3-031-37007-6_15
- Mumin Adhami, Mateo Garcia-Sandoval, Thienan Hoang, Matthew Whetham, Can Sun, Austin R. J. Downey, Yanzhou Fu, and Lang Yuan. Design of vacuum- and pressure-compatible optical and thermal camera modules for laser powder bed fusion. In H. Felix Wu, editor, Nondestructive Characterization and Monitoring of Advanced Materials, Aerospace, Civil Infrastructure, and Transportation XX, page 16. SPIE, April 2026. doi:10.1117/12.3090848
- Austin Downey and Laura Micheli. Vibration mechanics: A practical introduction for mechanical, civil, and aerospace engineers. January 2026. doi:10.31224/6182

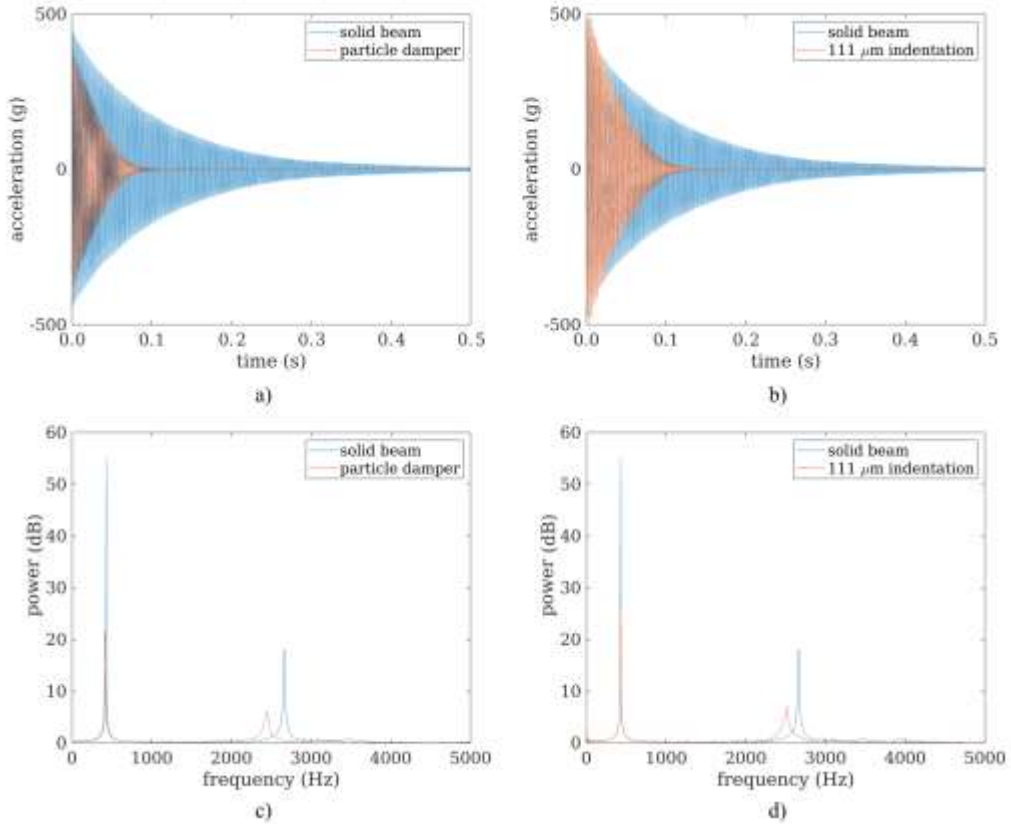
AI tools assisted with image creation, text editing, and presentation structure and storyboarding.

Prior Work in Particle Dampers

Fu et al. (2023): Compression of Particle-Damper Pockets in LPBF Beams

Scope of the study:

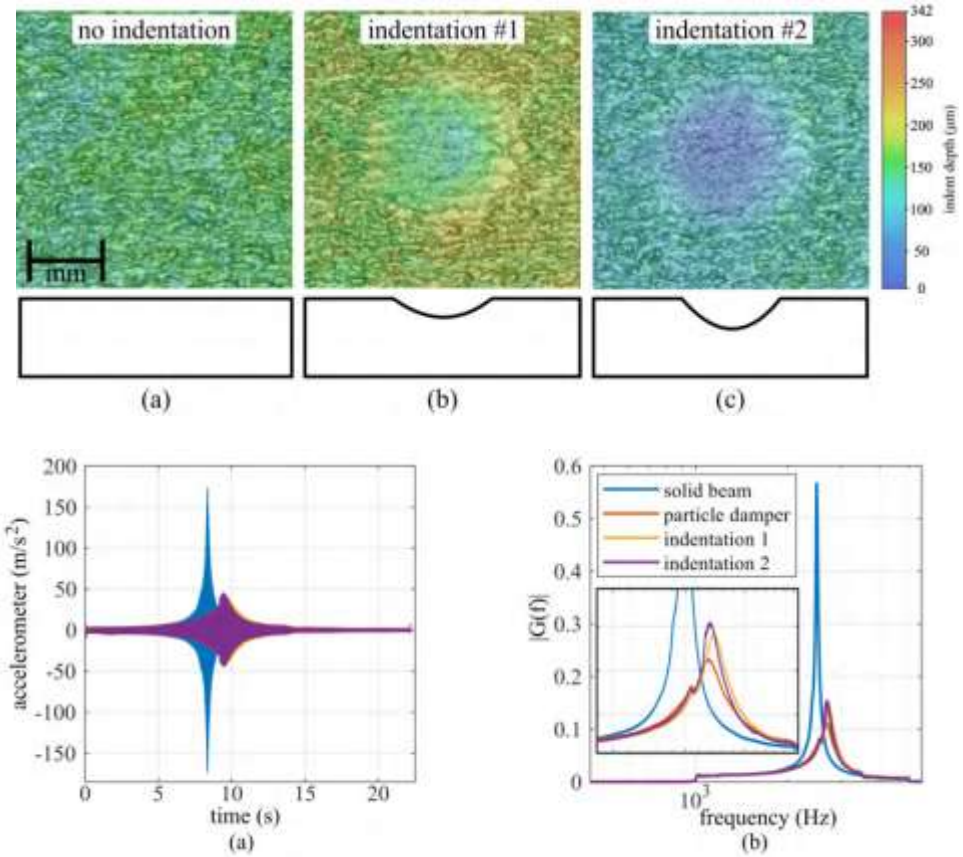
- Investigated LPBF 316L cantilever beams with powder-filled cavities and three post-print indentation levels. Shock tests quantified acceleration decay, FFT response, damping ratio, and Q factor.
- Examined isolated cantilever beams, not PCB-mounted heat sinks. The study did not test whether an integrated particle damper mitigates electronics-assembly shock while maintaining thermal performance.



Satme et al. (2024): Particle Packing Density and Frequency Response

Scope of the study:

- Studied how post-print indentation changes particle packing density and harmonic vibration response of LPBF cantilever beams. Shaker tests and a transfer-function model characterized modal attenuation.
- Focused on continuous excitation of individual beams, without evaluating transient shock loading or combined thermal–dynamic behavior of a PCB-mounted heat sink.



Satme et al. (2026): Tunable LPBF Damping via Post-Print Compaction

Scope of the study:

- Combined shock and shaker testing of LPBF 316L particle-damped beams, supported by transfer-function modeling and FEM. The unindented damper reduced Q factor (degree of underdamping in an oscillator) from 174.8 to 116.73. A higher Q value indicates lower energy dissipation.
- Demonstrated tunable damping in cantilever beams, but did not assess a functional heat sink performing both thermal management and shock mitigation within a PCB assembly (approximately 33%).

